Biophysical Chemistry 253 (2019) 106218

Contents lists available at ScienceDirect

Biophysical Chemistry

journal homepage: www.elsevier.com/locate/biophyschem

Fluorescence correlation spectroscopy as a tool for the study of the intracellular dynamics and biological fate of protein corona

Marta Martinez-Moro, Desiré Di Silvio, Sergio E. Moya*

Soft Matter Nanotechnology Laboratory, CIC biomaGUNE, Paseo Miramón 182 C, 20014 San Sebastian, Spain

HIGHLIGHTS

- Proteins interact with nanomaterials adsorbing on their surface and developing a corona.
- Protein corona changes the biological identity of nanomaterials, affecting their biological fate.
- FCS/FCCS provide unique information on the formation, stability and dynamics of the protein corona *in situ*.
- FCS/FCCS allow the study of the protein corona in complex biological environments such as cells in real time.

GRAPHICAL ABSTRACT

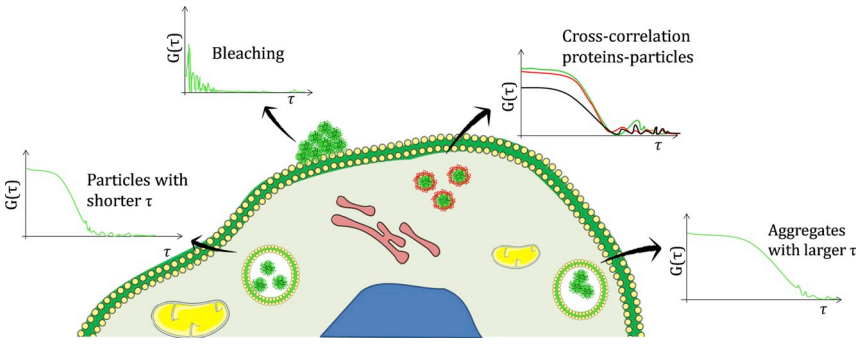

ARTICLE INFO

Keywords:
Protein corona
Biological fate
Fluorescence correlation spectroscopy
Fluorescence cross-correlation spectroscopy

ABSTRACT

In biological fluids, nanoparticles (NPs) are in contact with proteins and other biomolecules. Proteins adsorb to NPs and form a coating called a protein corona (PC). The PC is known to greatly affect the interaction of NPs with biological systems. A comprehensive knowledge of the protein nanoparticle interaction is essential to understand the biological fate of NPs and for the design of NPs for biomedicine. Fluorescence correlation spectroscopy (FCS) and fluorescence cross-correlation spectroscopy (FCCS) are sensitive spectroscopy techniques that measure fluorescence intensity fluctuations of single molecules inside a femtoliter confocal volume. Both techniques are suitable for studying the formation of protein corona around NPs and for examining corona stability *in situ* in biological matrixes. In this review we provide a short description of FCS/FCCS and their application in PC studies, highlighting results from our work about the impact of surface chemistry of NPs on corona formation and NP intracellular fate.

1. Introduction

The study of the biological fate of nanomaterials and their interaction with biomolecules is fundamental for improving the performance of these materials in biomedicine and for understanding toxicological end points. The nanomedicine market is estimated to value up to $350.8 billion by 2025 [1], but despite the huge amount of investment, there is still poor translation of nanomaterials from *in vitro* to *in vivo* applications. It was recently highlighted that in the past 10 years of working on nanoparticles (NPs) for drug delivery, a low delivery efficiency has been achieved, with only 0.7% of the doses of NPs injected reaching the tumour site [2]. In this regard, understanding interactions between NPs and biomolecules is of fundamental importance. Of particular value, is gaining deeper insight into the key role

* Corresponding author.
E-mail address: smoya@cicbiomagune.es (S.E. Moya).

https://doi.org/10.1016/j.bpc.2019.106218
Received 18 June 2019; Accepted 3 July 2019
Available online 04 July 2019

of the biomolecular protein corona (PC), which has been widely acknowledged as pivotal in providing a biological identity to nanomaterials [3,4]. In this short review we aim to discuss the use of fluorescence correlation spectroscopy (FCS) for characterizing protein corona nanomaterial *in situ* in extremely complex environments such as live cells.

FCS is a fluorescence based technique that gives information on the diffusion of fluorescent molecules or objects. From the diffusion times, the size of diffusing species can be determined, and the interaction among molecules or nanoparticles can be studied. Using fluorescently labelled nanomaterials or proteins, it is possible to study protein corona formation with FCS by recording the changes in diffusion of the labelled species before and after corona formation. Moreover, using nanomaterials and proteins each labelled with dyes without overlapping spectra allows for the cross correlation of the two colours, which provides information on the stability of the corona and the exchangeability of the proteins forming the corona (fluorescence cross-correlation spectroscopy). Moreover, FCS allows for studies inside cells and provides information on how intracellular nanomaterial translocation affects PC. Besides corona formation and stability, FCS can also provide data on the state of aggregation of the nanomaterials in the presence of proteins. In our group we are interested in correlating the surface chemistry of nanomaterials with PC formation and stability. We will present some examples from our work on how the aggregation and intracellular dynamics of nanomaterials are affected by the formation and evolution of PC, and ultimately by the chemistry of the nanomaterials.

1.1. The protein corona

Biomolecular corona is defined as the entity resulting from the spontaneous interaction of nanomaterials with biological matter [5,6]. It is a dynamic entity that forms within 30 s [7] and evolves with time. Initially, the most abundant proteins such as albumin, bind to the NPs, but later on they are partially replaced by less abundant proteins that have a higher affinity for the NP surface [8]. The PC composition depends on the physical-chemical properties of the nanomaterial such as size, shape, coating, and surface charge [9–13], and on the environment, including biological milieu, pH, time of exposition, temperature, and shear stress [14–18]. PC structure has been described as being constituted of two layers: the closest protein layer to the NP surface is called hard corona (HC) with proteins tightly bound to the NPs. Once formed, the HC is very stable over time [19]. Around the HC there is another layer of proteins that are weakly bound to it. These proteins form like a cloud around the HC and exchange fast with the surrounding biomolecules. This weak corona is called soft corona (SC) [20]. While the HC has been described in detail because it is easy to isolate, the characteristics of SC are largely unknown, with limited information available on its composition, binding affinity, and structure [21]. This knowledge gap is notable because, as depicted in the current accepted model for PC NPs (Fig. 1), the SC is the most external layer at the interface and is thus very important in nano-bio interactions.

1.2. The biological relevance of the protein corona

The biomolecular corona confers a new biological identity to the NPs that modifies the way they behave in biological matrixes. At first, the formation of the protein corona affects the colloidal stability of the NPs. A pre-formed corona has been shown to be a way of limiting NP agglomeration in biological fluids due to high ionic strength, whereas it has been reported to induce agglomeration in other cases [22]. A corona enriched with a particular protein, besides providing additional stability, might also provide the NPs with a targeting moiety [23]. A targeting moiety can prevent non-specific uptake, thus prolonging NP half-life in the blood stream and increasing the potential delivery to the desired site (*e.g.* apoliproteins) [24]. However, it is also possible that the PC can interfere with targeting properties by masking the NP coating [25,26]. PC formation can impact cell cytotoxicity, nanomaterial uptake and trafficking inside the cell [27]. It is well known that graphene and carbon nanotubes [28,29] are highly toxic for cells because they are able to disrupt and penetrate the cellular membrane. Quantum dots become highly toxic when the metal core is exposed [30]. The PC constitutes a natural coating, limiting the interaction of NPs with the membrane and reducing the damage induced by direct exposure of the cells to those nanomaterials. On the other hand, when proteins are adsorbed to the NP surface, they might face denaturation and expose epitopes that trigger anti-inflammatory or auto-immune responses [31] as has been reported for fibrinogen on Au-NPs coated by poly(acrylic) acid [32]. Extrinsic factors influencing the PC around NPs include the media composition, protein gradients and blood pressure [33–35]. The study of PC in real time and in dynamic conditions such as those encountered *in vivo* is of great importance toward understanding PC formation and evolution.

2. *Ex-situ vs in situ*

Predicting PC formation and evolution is fundamental for fully exploiting its potential. Corona formation can be studied using *ex-situ* and *in situ* techniques. *Ex-situ* techniques require isolation and purification of the protein corona from the initial media. Although valuable information might be obtained, especially on PC composition, samples are manipulated and do not represent quite the same entity that originally was. *In situ* techniques have the advantage that PC around NPs can be studied in the original environment. However, tracing nanomaterials in biological matrixes is always challenging. Some techniques used for visualization and quantification of nanomaterials in biological matrixes require the fixation and destruction of the biological material, such as Transmission Electron Microscopy (TEM) and cryo-TEM [36,37], or Inductively-Coupled Mass Spectroscopy (ICPMS) [38]. The intracellular location of NPs and PCs and protein concentration are rather important aspects to determine the fate of NPs in living organisms and cells. *In vivo* ultra-highly sensitive imaging techniques for radioisotopes such as Positron Emission Tomography (PET) or Single-Photon Computed Tomography (SPECT) allow for real time and quantitative determination of radiolabeled nanomaterials [24,39]. While NP biodistribution can be followed by PET/SPECT techniques, the study of the protein corona *in vivo* has been performed after blood recovery and PC NP purification. In the cellular environment, fluorescence and Raman techniques are preferred for NP localization and to trace the fate of the corona. Confocal Laser Scanning Microscopy (CLSM) and Confocal Raman Microscopy (CRM) have enough resolution to resolve different regions within fixed and live cells and to visualize NPs, after fluorescence labelling in the case of CLSM and from characteristic Raman bands for CRM. CLSM provides more detailed and direct information on the intracellular localization of nanomaterials than Raman microscopy as intracellular compartments can be selectively labelled [40]. In addition to CLSM, other fluorescence techniques can be applied for tracing nanomaterial fate at cell level. Flow cytometry is used to quantify the uptake of nanomaterials per cell and to follow uptake kinetics [41]. Total Internal Reflection Fluorescence (TIRF) microscopy can be used to trace membrane translocation of nanoparticles [42,43]. FCS is a technique based on recording fluorescence fluctuations in a confocal volume, which are related to the diffusion of the fluorescent molecules. Diffusion times can be correlated with the size of the diffusing species, and also with the local micro-environmental conditions. The technique offers a spatial and temporal resolution that is far superior to that obtained with most of the techniques mentioned thus far. FCS can provide quantitative values for the NP concentration, the state of nanomaterial aggregation, and information on the local environment of nanomaterials based on measuring their diffusion coefficient. As is the case with nanomaterial aggregation, the formation of the protein corona around NPs results in a larger object with longer diffusion time. If proteins and NPs are each labelled with a

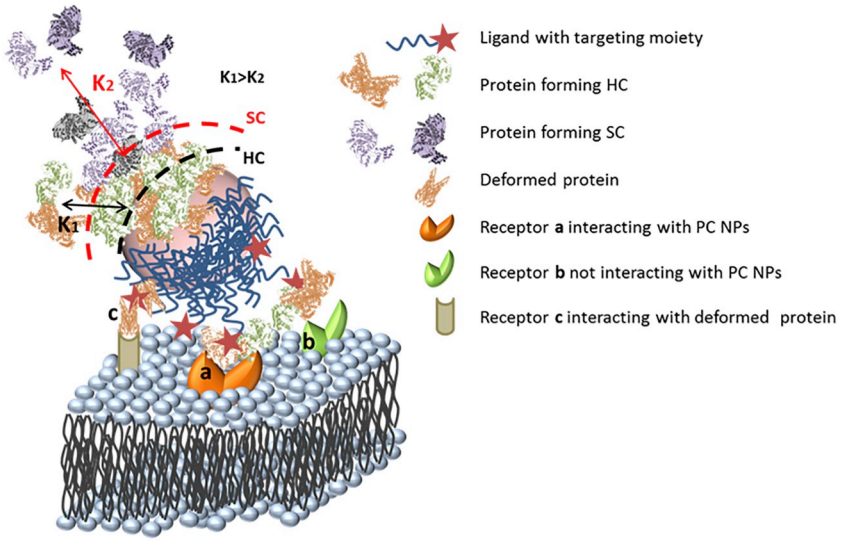

Fig. 1. NP coated by protein corona. The black dashed line represents the hard corona (HC) and the red dashed line the loose soft corona (SC). Proteins in the HC and SC are bound respectively with affinity coefficients K_1 and K_2, with K_1 being greater than K_2. The protein corona can enhance the interaction of the NP with membrane receptors (a), hinder it (b), or create unexpected interactions (for example, caused by proteins that can change confirmation upon binding the NP surface (c)). (For interpretation of the references to colour in this figure legend, the reader is referred to the web version of this article.)

different dye with no spectral overlap between them, the interaction between the nanomaterial and the proteins can be studied by Fluorescence Cross-Correlation Spectroscopy (FCCS). FCCS is a variant of FCS, where the fluorescence fluctuations of two fluorescent objects are cross-correlated in time.

Both FCS and FCCS allow real time measurements and can be applied not only in bulk, but also intracellularly in combination with CLSM. These features make FCS techniques a unique tool for studying the dynamics of nanomaterials at cell level. Issues such as the state of nanomaterial aggregation or degradation, and the interaction of NPs with biomolecules can be fully monitored by FCS techniques intracellularly. This monitoring provides insight into how cells process nanomaterials, and is highly relevant for toxicological studies and nanomedicine.

3. Fluorescence correlation spectroscopy (FCS) and fluorescence cross-correlation spectroscopy (FCCS)

3.1. Fluorescence correlation spectroscopy

Fluorescence correlation spectroscopy [44,45] is a spectroscopic technique based on the record of the fluorescence intensity fluctuations inside a femtoliter confocal volume. It is a very sensitive technique whose optimal ratio of signal to noise occurs when a low concentration of particles, in the nanomolar range, are diffusing in the confocal volume.

Intensity fluctuations are the deviation of the signal from its temporal average fluorescence [46].

$$\delta I(t) = I(t) - \langle I(t)\rangle \tag{1}$$

$$\langle I(t)\rangle = \frac{1}{T}\int_0^T I(t)dt \tag{2}$$

This fluorescence signal is recorded in a correlator obtaining the autocorrelation function (ACF or G(τ)).

$$G(\tau) = \frac{\langle I(t)I(t+\tau)\rangle}{\langle I(t)\rangle^2} \rightarrow G(\tau) = \frac{\langle \delta I(t+\tau)\delta I(t)\rangle}{\langle I(t)\rangle^2} + 1 \tag{3}$$

We are able to determine the fluorescence signal I(t) and its fluctuation δI(t) with the detection efficacy of the setup and the concentration of the sample on the space of the observed volume ($\vec{r} = (x,y,z)$) as:

$$I(t) = \kappa \int_V I_s(\vec{r})\cdot S(\vec{r})\cdot CEF(\vec{r})\cdot C(\vec{r},t)d\vec{r} \tag{4}$$

$$\delta I(t) = \kappa \int_V I_s(\vec{r})\cdot S(\vec{r})\cdot CEF(\vec{r})\cdot \delta C(\vec{r},t)d\vec{r} \tag{5}$$

κ detection efficacy.
I_s excitation energy.
$CEF(\vec{r})$ collection efficiency function of the system.
$S(\vec{r})$ optical transfer function objective-pinhole.
$C(\vec{r},t)$ distribution of fluorophore.

Substituting eq. (4) and eq. (5) in eq. (3), the correlation function can be written as

$$G(\tau) = \frac{\iint I_p(\vec{r})I_p(\vec{r}')S(\vec{r})S(\vec{r}')CEF(\vec{r})CEF(\vec{r}')\langle \delta C(\vec{r}',t+\tau)\delta C(\vec{r}',t)d\vec{r}d\vec{r}'\rangle}{\langle C\rangle^2\left(\int I_p(\vec{r})\cdot CEF(\vec{r})\,d\vec{r}\right)^2} + 1 \tag{6}$$

To simplify eq. (6), we take into account the confocal setup where the pinhole removes the light out of the focus and the intensity is maximized in the center of the beam in the focal plane.

$$\omega(\vec{r}) = I_p(\vec{r})\cdot S(\vec{r})\cdot CEF(\vec{r}) = cte\cdot e^{-2x^2/w_0^2}e^{-2y^2/w_0^2}e^{-2z^2/z_0^2} \tag{7}$$

Where w_0 and z_0 are the distance where the intensity decay $1/e^2$.

The solution of eq. (6) gives us the correlation function:

$$G(\tau) = \frac{1}{N}\left(1+\frac{4\tau D}{w_0^2}\right)^{-1}\left(1+\frac{4\tau D}{z_0^2}\right)^{-1/2} + G_\infty \tag{8}$$

D diffusion coefficient.
N number of particles.
G_∞ offset of the correlation function.
τ diffusion time.

The first part of eq. (8) refers to the average of particle numbers in the confocal volume. It is defined as the volume that contains N fluorophores at a known concentration. From calibration measurements, knowing the diffusion coefficient of the fluorophore it is possible to determine the confocal volume [47]. The size of the confocal volume is really important to detect single molecules because the fluctuations decrease as the number of objects increases. A suitable number of objects is between 0.1 and 1000 nM corresponding to a diffraction focal volume $<$ 1 fL. [48–50]

The number of objects and the concentration in the confocal volume (V_{eff}) can be determined from the amplitude of the correlation function at $t = 0$:

$$G(0) = \langle N\rangle^{-1} \tag{9}$$

The concentration of particles is given by:

$$\langle N \rangle = V_{eff}\,[C] \tag{10}$$

On the other hand, from the diffusion coefficient D of the species, it is possible to calculate the hydrodynamic radius with the Stokes-Einstein equation

$$D = \kappa_B T\,(6\pi\mu r_H)^{-1} \tag{11}$$

κ_BBoltzmann's constant.
T Absolute temperature.
μ viscosity of the medium.

3.2. Fluorescence cross-correlation spectroscopy

Fluorescence cross-correlation spectroscopy [51] is a variation of FCS. This technique studies the interaction between two species labelled with two spectroscopically different fluorophores [52]. The binding between the species conveys a longer diffusion time and hence, a decrease in the diffusion coefficient. The cross-correlation is sensitive to the signal of the molecules with the two labelled species so it is easy to measure interactions between proteins [53] and other biomolecules [54] not only in solution, but also in cells [55].

The eq. (3) changes to:

$$G(\tau) = \frac{\langle I_a(t) I_b(t+\tau)\rangle}{\langle I_a(t)\rangle \langle I_b(t)\rangle} \tag{12}$$

where *a* and *b* are the two differently-labelled species.

The concentration of the bound species could be determined by the amplitudes of the auto and cross-correlation curves at time zero:

$$\frac{G_{ab}(0)}{G_a(0)\cdot G_b(0)} = \langle C_{ab}\rangle V_{eff} \tag{13}$$

Despite FCS being discovered in 1972 [44,45], this technology only started to emerge in 1993 with the implementation of confocal microscopy for individual molecule measurements [56]. The instrumentation for FCS/FCCS is based on a confocal setup (Fig. 2).

3.3. FCS and FCCS: state of the art

In FCS, the movement of labelled species in and out of the confocal volume is recorded. The diffusion time is dependent on the size of the diffusing species and it can be used to study aggregation or association of molecules and nanoparticles. The association between labelled species with itself or with unlabeled species will result in a measured diffusion time that is longer than that of the single dispersed molecule. The interaction can be monitored in real time until equilibrium is reached [58–61]. In this way, from the analysis of the autocorrelation function (ACF), it is possible to take additional information such as the equilibrium constant or the concentration of a labelled sample. Furthermore, changes in the diffusion time have been associated with conformational changes of proteins [62]. Intracellularly, FCS has been employed to measure the concentration of labelled species [47,63–65], their interaction with the cell membrane [66], their dynamics [67–69], or even their cellular internalization [70].

FCCS can complement FCS data and is particularly useful to study the formation of molecular complexes in solution and intracellularly [53,55,71,72]. The fundamental condition for using FCCS is that the two species under investigation and forming the complex are labelled by two different fluorescent labels whose fluorescence spectra do not overlap. Then, if the particles diffuse together in the confocal volume, the simultaneous recording of their fluorescence will generate a cross-correlation function different from zero (Fig. 2-II and 2-III).

3.3.1. Protein corona studies by FCS

One interesting application of FCS is the study of protein corona formation and dynamics *in situ*. [73,74] In biological environments, nanoparticles can adsorb different biomolecules including proteins, lipids and sugars. Due to this association, the size of the nanoparticles usually increases and consequently, their diffusion time also increases. This change in diffusion time can be detected by FCS provided that the NPs or the biomolecules are labelled with a fluorescent dye. FCS and FCCS allow *in situ* measurements without the need for additional steps such as centrifugation, or filtration that are required to separate the NP with the PC from the rest of the biomolecules present.

The most abundant protein in blood is the albumin, which is usually used as a model for whole plasma [75]. Röcker et al. [76] studied the association between human serum albumin (HSA) and FePt NPs coated with a red-labelled amphiphilic polymer. The polymer displayed carboxylic groups that provided a negative surface charge that favors protein binding. The authors showed that when the HSA concentration increased up to physiological conditions (800 μM), HSA formed a monolayer on the NP surface and the diffusion time increased until saturation. Different kinetics parameters such as Hill's constant and the dissociation coefficient were obtained. CdSe/ZnS quantum dots (QDs) functionalized with a similar amphiphilic polymer were used for comparative studies. A protein monolayer is formed on the surface but a weaker interaction with QDs is observed with a larger dissociation coefficient. Similar experiments were performed for human transferrin (TF) only with FePt particles [77]. It was demonstrated that TF keeps binding to the NP surface until a monolayer is formed up to a maximum concentration of 26 μM, very similar to the TF blood concentration (30 μM). This protein interacts with specific receptors on the cell membrane and has a lower affinity for FePt NPs than HSA because of the charge of their residues. Authors show that protein affinity for NP surface depends on the primary and secondary structures of the protein [78]. FCCS was applied to study the interaction of nanoparticles with HSA, and ApoA-I and ApoE4 proteins, which are responsible for the transport of lipid molecules as cholesterol. A clear dependence is observed between protein concentration and hydrodynamic radius. As in previous studies, once the particles and proteins reached equilibrium, no more proteins bind on the surface. The number of molecules attached to the surface was calculated by ACF analysis. Twenty-seven molecules of HSA, 50 of ApoA-I and 65 of ApoE4 were found per nanoparticle. Nonetheless Hill's constant was higher for ApoE4 than for HSA and ApoA-I indicating that it has a higher affinity for the NP surface. The reason for this higher affinity is likely due to the ApoE4 conformation, which exposes many positive charges to the bulk.

An interesting study conducted by FCS by Hühn et al. [79] in 2017 showed that gold NPs coated by a positive and a negative polymers have similar affinity for HSA. This finding seems to contradict the expectation that the superficial charge of a NP is the main determinant for PC composition [80], but the results may be due to the exchange between the different proteins in serum. Another explanation proposed is that the low charge density in the negative polymer causes a reduction in the adsorption of proteins. A common coating employed for reducing the adsorption of proteins is polyethylene glycol (PEG). PEGs with different molecular weights and surface densities possess different stealth abilities. In particular it has been shown that the best reduction in terms of protein absorption was achieved by 5 K MW PEG with a surface density of 5% wt. [81] With non-PEGylated NPs, FCS experiments showed that a HSA monolayer formed with a thickness of 3 nm; PEGylated particles also increased in size, but only by 1.5 nm. The deposition of HSA on PEGylated NPs was explained by the partial penetration of HSA in the PEG shell [82].

FCS was used to elucidate the dynamic nature of the protein corona [83]. The adsorption kinetics of proteins was studied with HSA-coated silica NPs in the presence of labelled fibronectin (FIB). The results showed that FIB adsorption on the NP surface depends on the HSA concentration. For the highest HSA concentration (10 mg/mL) the diffusion time and the time to reach the FIB adsorption saturation increase respect to the uncoated particles. Using TF instead of HSA, FCS shows similar binding affinity for FIB.

It was previously shown that HSA binds the NP surface with its

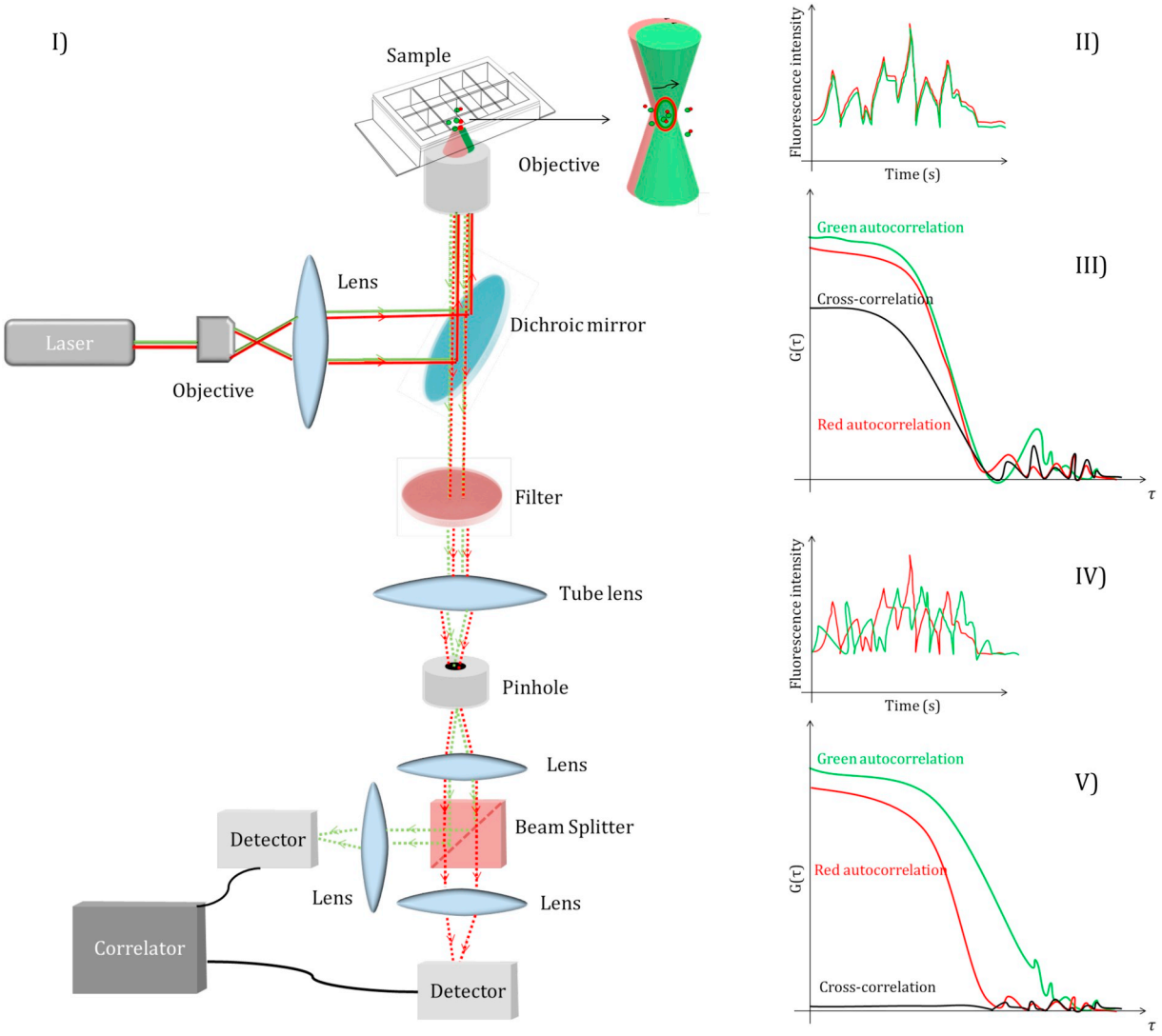

Fig. 2. I) Scheme of FCS/FCCS setup. Fluorescence correlation (green) and cross-correlation spectroscopy setup (red and green). The excitation sources are lasers with the desired wavelength. They are aligned to the same confocal volume but not overlapping. The two signals are separated by filters and a dichroic mirror, and go through an objective to focus into the sample. The fluorescence is collected by the same objective, separated from the excitation light by the dichroic mirror and focused by the tube lens in a pinhole. This pinhole collects only the fluorescence from the focal plane that arrives to the detectors for correlation analysis. In the case of FCCS, only if the two species interact and diffuse together in the confocal volume (II), will the correlation between both signals result in a cross-correlation (III) [57]. Otherwise, the count rate graphs not match (IV) and the correlation function will be zero (V). The correlograms obtained give information not only of the diffusion time, but also of the concentration of the sample. Once the signal is obtained, different software packages can be used to fit the data and obtain the diffusion coefficient or the diffusion time of the measurements, as well as the number of particles inside the confocal volume. (For interpretation of the references to colour in this figure legend, the reader is referred to the web version of this article.)

triangular face. [76] Studies of FCS highlighted that changing the polarity of some residues of HSA, causes alteration of the protein secondary structure and consequently the nature of the interactions with the NPs. [84] In this case, experiments were performed with dihydrolipoic acid-coated CdSe/ZnS quantum dots. HSA was functionalized with two different compounds, succinic anhydride (HSA-su) to provide a negative charge and separately with ethylenediamine to provide a positive charge (HSA-am). HSA-am gave a shorter diffusion time than the HSA-su because of its higher affinity for dihydrolipoic acid-coated CdSe/ZnS quantum dots. Besides, simulation studies show that protein modification caused a rearrangement in the orientation adsorption producing an increase in the hydrodynamic radius in the case of HSA-su.

The effect of external factors on PC morphology was studied using bovine serum albumin (BSA) interacting with carboxylated ZnS/CdSe (QDs) [85]. Different temperatures and pH were considered. The decrease in the thickness of PC with the temperature was reflected by an increase in the dissociation constant. Changes in pH affect the isoelectric point of BSA. FCS measurements confirmed that at pH 7.4 there was less interaction of BSA with negatively charged particles because BSA global charge was negative.

3.3.2. *Intracellular protein corona studies*

One of the strengths of the FCS is the possibility to work in extremely complex environments such as that encountered inside cells. In cells, everything will be invisible for FCS except for the fluorescently labelled species. The combination of FCCS with CLSM permits joining imaging with the study of the diffusion properties of the object under investigation in real time.

Seminal work by Bacia et al. on the translocation and fate of proteins intracellularly combined CLSM and FCCS to show the endocytic pathway of cholera toxin (CTX) from the cell membrane to the Golgi apparatus and its subsequent degradation [86]. CTX was formed by two subunits which were labelled with fluorophores with different emission

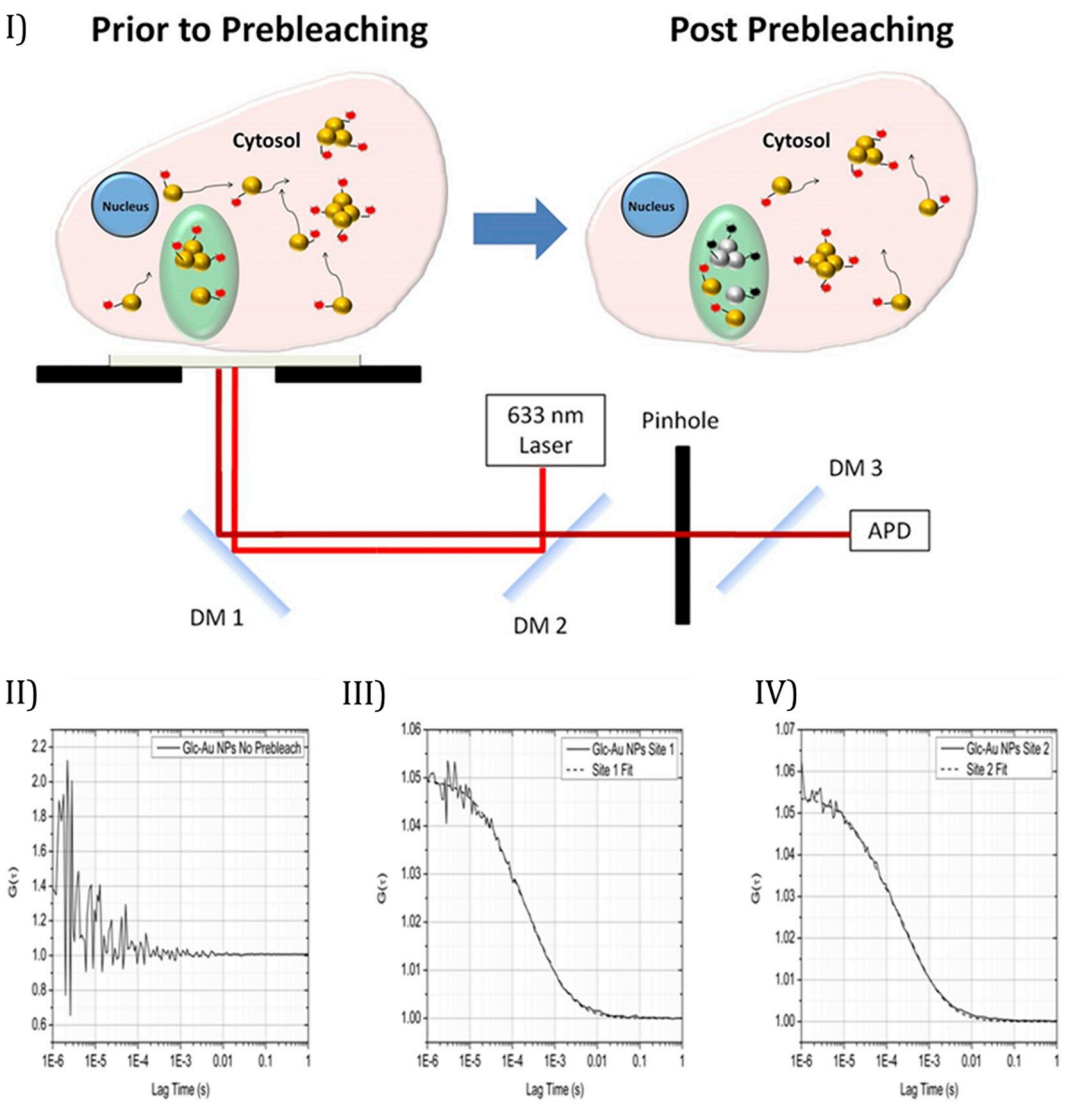

Fig. 3. I) Representation of the intracellular uptake before and after bleaching [50] II) ACF of large aggregates prebleaching. III) and IV) ACF for two different sites of the cell in the CLSM image after bleaching. Murray RA, Qiu Y, Chiodo F, Marradi M, Penadés S, Moya SE.: A quantitative study of the intracellular dynamics of fluorescently labelled glyco-gold nanoparticles via fluorescence correlation spectroscopy Small. 2014. 10. 2602-10. Copyright Wiley-VCH Verlag GmbH & Co. KGaA. Reproduced with permission.

spectra to study their separation by cross-correlation. Once the complex arrived to the Golgi apparatus, no cross-correlation was observed, implying dissociation of the two subunits.

One of the few examples of NP-cell investigations by FCS was reported by Murray et al. [70] Gold NPs coated with fluorescent glucose were studied *in vitro* in different media by FCS. Diffusion time increases when the particles are in cell media, which means a larger hydrodynamic radius (typically the double). When the NPs are internalized in HepG2 cells, they form big aggregates with their diffusion time exceeding the technique limit. A pre-bleaching step was used to overcome the masking of the fluorescent signal of smaller fluorescent species by big aggregates. The measured diffusion times revealed the association of the particles with different biomolecules or parts of the cell. The measurements were performed in different positions in the cell and a homogeneous distribution was observed (Fig. 3-II, 3-III, and 3-IV).

Our group has focused on studying the interaction between proteins and NPs coated with molecules with different affinity for proteins. PEG is the most widely used coating to avoid non-specific interactions with proteins, although some concerns about its safety have been raised [87]. For this reason, new stealth molecules are being investigated that minimize the interaction of the particles with proteins, prolonging NP blood half-life. Silvestri et al. functionalized gold nanoparticles with mercaptosuccinic acid (Au-MSA), N-4-thiobutyroil glucosamine (Au-glucosamine), Au-PEG5000 and Au-Alkyl-PEG600, and studied the interaction of the NPs with proteins of cell media and their internalization in A549 cells. Protein-free cell media studies confirmed the low affinity of PEGylated NPs for proteins [82]. Conversely, Au-MSA and Au-glucosamine experienced an increase in their size up to 40 nm possibly due to aggregation as a consequence of the higher ionic strength encountered in the cell media compared to water. Addition of fetal bovine serum induced a decrease in the hydrodynamic radii because of the additional stability provided by the proteins. Once internalized in cells, the NPs aggregated and formed large structures with intracellular proteins and organelles. Different parts of the cells were investigated by FCS (Fig. 4-I). The diffusion times of fluorescent aggregates were clustered into four different groups: $500 < \tau_D(\mu s) < 1500$; $1500 < \tau_D(\mu s) < 3000$; $3000 < \tau_D(\mu s) < 6000$ and $\tau_D(\mu s) > 6000$. A combination of FCS with CLSM allowed determination of a heterogeneous distribution of the NPs in the cell compartments with a wide distribution of diffusion times (Fig. 4-II-A y 4-II-B). After a one hour incubation, Au-MSA and Au-glucosamine showed large diffusion times probably because of their interaction with different cell molecules. For

I)

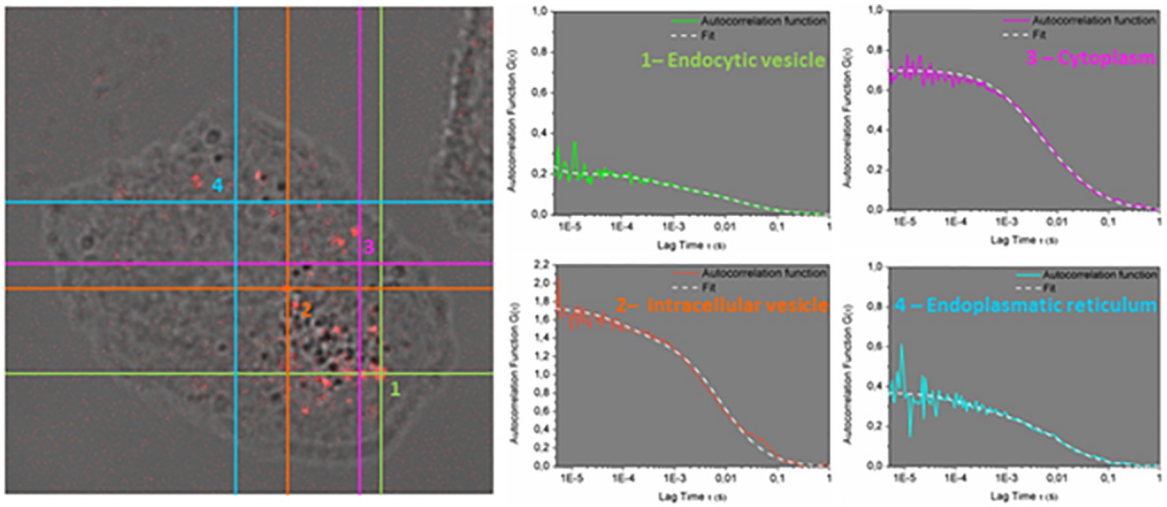

II)

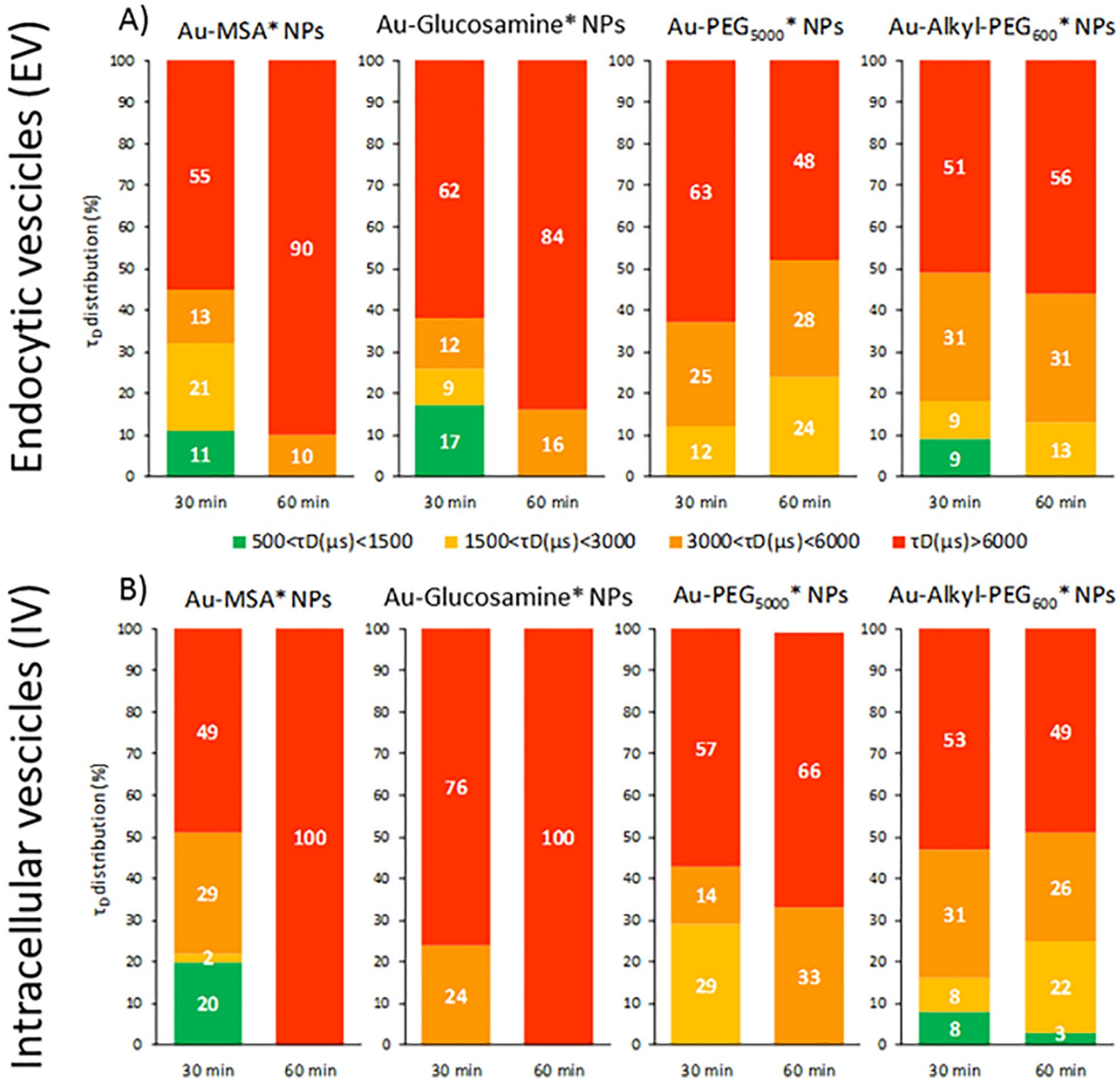

(caption on next page)

Fig. 4. Au NP uptake followed by CLSM and FCS in A549 cells. NPs were coated with mercaptosuccinic acid (Au-MSA), N-4-thiobutyroil glucosamine (Au-Glucosamine), HS-PEG500 (Au-PEG5000) and HS-Alkyl-PEG600 (Au-Alkyl-PEG600) and labelled by ATTO550. I) Representative confocal image of an A549 cell incubated with Au-MSA* NPs as a combination of the transmission and fluorescence channels and FCS correlograms measured in the marked area in the confocal micrograph. FCS correlograms were fitted with a normal diffusion 3D double exponential model. II) Percentage distribution of the more representative diffusing species obtained fitting tracks ($n > 30$) by a 3D normal diffusion model with 2 components. The diffusion times obtained were grouped into four classes ($500 < \tau D$ (μs) < 1500; $1500 < \tau D(\mu s) < 3000$; $3000 < \tau D(\mu s) < 6000$ and $\tau D(\mu s) > 6000$). Results for Au-MSA* NPs, Au-Glucosamine* NPs, Au-PEG5000* NPs and Au-Alkyl-PEG600* are reported at 30 and 60 min of incubation. A) Endoplasmatic vesicles; B) Intracellular vesicles. (figure from Ref [87] reproduced with permission of publisher)

PEGylated particles it was still possible to find NPs with diffusion times below 6000 μs. In particular, a population of Au-Alkyl-PEG600 with diffusion times between 500 and 3000 μs could be measured. We believe that the lower binding affinity of Au-Alkyl-PEG600 for proteins *in vitro*, can be related to a significant decrease in its aggregation intracellularly.

We have also used FCCS to carry out affinity studies and to describe PC fate once NPs are translocated into cells. For these studies we have used NPs with either a PC formed by proteins with specific affinity for the NP surface coating, or with a non-specific BSA-coating [88]. Studies were performed with gold NPs functionalized with the glucosamide ligand and labelled with BSA and Concanvalin A (Con A), which has a specific interaction with glucosamine in presence of Ca^{+2} ions. The two proteins, BSA and Con A, have similar diffusion times in solution of around 800 μs. For the protein exchange study, first the protein corona was formed with unlabeled BSA and followed by exposure to a labelled Con A, and then repeated *vice versa*. Analyzing the cross-correlation function, it is possible to know if one of the protein is retained in the protein corona in presence of an excess of the other protein (Fig. 5-I). If the labelled proteins and NPs diffuse in the confocal volume at the same time, it means they are cross-correlated and the cross-correlation function (CCF) will be higher. Conversely, if exchange takes place, there will be less labelled protein on the PC and the CCF will be lower. For the NPs with BSA PC exposed to labelled Con A, the amplitude of the CCF increases with time, reaching 53% of the Con A associated with the BSA PC after 2 h. When BSA is the labelled protein and Con A is not labelled, the CCF amplitude decreases close to zero with time, meaning that the BSA is substituted by Con A in the protein corona. After exchange studies, the particles were incubated with A549 cells. In the case of the particles coated with BSA (black bars in Fig. 5-I), large aggregates and lower CCF were measured. CCF intracellularly decreases over time, leading to the hypothesis that the protein corona is lost with time. For NPs with Con A PC (white bars in Fig. 5-II) CCF remains high and constant for 24 h inside the cell. After 24 h the NPs are too aggregated for FCS studies. The diffusion time of the particles is so large that the FCS is not able to resolve it. FCCS shows that the strength of the interaction between NPs and proteins is retained after NP translocation, which may potentially affect NP trafficking.

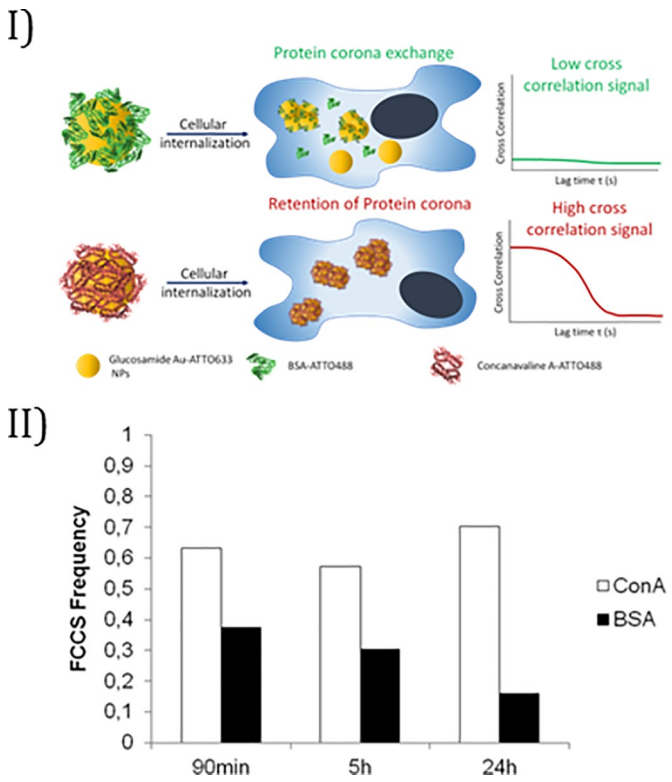

Fig. 5. I) Scheme of the protein exchange cross-correlation signal. II) FCCS frequency over time for measurements carried out with pre-formed BSA and Con A PC NPs incubated in A549 cells. (Fig.5 II from Ref. [88] reproduced according to: https://creativecommons.org/licenses/by/4.0/))

3.4. Advantages and limitations

Fluorescence correlation and cross-correlation spectroscopy provide information on a wide range of processes including the PC formation in bulk and in cells. They are highly sensitive techniques that provide information about single molecule processes. Small amounts and low concentrations of fluorescent species, in the nanogram and nanomolar range, are needed and the sample and cells are not destroyed during the experiment. FCS and FCCS techniques provide a perfect tool to study PC formation and follow the biological fate of particles *in situ* without the need for washing steps or a minimum spatial proximity like FRET experiments.

However, these techniques have some limitations. They record the fluorescence fluctuations in a confocal volume, which means that the species under study need to be mobile in the confocal volume and must be fluorescently labelled. It is important to choose the appropriate fluorophore for FCS experiments. Fluorophores must be photostable with limited bleaching [89]. Data analysis, especially in complex systems might be difficult and can be misinterpreted. As with all fluorescence-based techniques, appropriate control experiments are needed to rule out any interference from the environment. Quantitative analyses are sometimes difficult as a proper model is needed to fit the data. In the case of the FCCS, fluorophores need to be chosen with maximal spectral separation to avoid cross-talk [55]. Samples with a low binding affinity are not suitable for FCCS because they would require a higher amount of labelled species that would result in bleaching with decay in the fluorescence intensity and no signal [90]. Artifacts can be generated by the fluorophore or by the setup. It is possible to avoid fluorophore artifacts by choosing a suitable photostable fluorophore, avoiding high brightness, and preventing formation of aggregates. The setup limitations may be minimized by using a small confocal aperture and conducting a proper calibration to ensure that the two confocal volumes overlap.

3.5. Perspectives

FCS/FCCS are excellent tools for studying the dynamics of NPs and their interaction with biomolecules in bulk, inside cells and in 3D cultures. Despite relatively few studies, the technique has great potential for gaining insight into the interactions of NPs with proteins

intracellularly, which is important for biomedical application. Most FCS studies of PC are performed by preparing the corona in bulk. A fundamental aspect of PC that could be addressed with FCS/FCCS would be the study of the interaction of NPs with specific proteins from the cell. Future work will require the expression of specific fluorescent proteins inside cells. FCS/FCCS can also provide information on the interaction of PC around NPs with other biomolecules such as other proteins, sugars, or lipids, which are also of key importance for understanding NP toxicity and for improving their potential in biomedical applications.

Acknowledgements

We thank the MAT2017-88752-R Retos project from the Ministerio de Economia, Industria y Competitividad, Gobierno de España for support. This work was performed under the Maria de Maeztu Units of Excellence Program from the Spanish State Research Agency – Grant No. MDM-2017-0720. We also thank Julia Cope, PhD of CIC biomaGUNE for providing editorial assistance for the manuscript.

References

[1] Nanomedicine Market Analysis By Products, (Therapeutics, Regenerative Medicine, Diagnostics), by Application, (Clinical Oncology, Infectious Diseases), by Nanomolecule (Gold, Silver, Iron Oxide, Alumina), & Segment Forecasts, 2018–2025, (2017).
[2] S. Wilhelm, A.J. Tavares, Q. Dai, S. Ohta, J. Audet, H.F. Dvorak, W.C.W. Chan, Analysis of nanoparticle delivery to tumours, Nat. Rev. Mater. 1 (2016) 1–12, https://doi.org/10.1038/natrevmats.2016.14.
[3] P. Jain, R.S. Pawar, R.S. Pandey, J. Madan, S. Pawar, P.K. Lakshmi, M.S. Sudheesh, In-vitro in-vivo correlation (IVIVC) in nanomedicine: is protein corona the missing link? Biotechnol. Adv. 35 (2017) 889–904, https://doi.org/10.1016/j.biotechadv.2017.08.003.
[4] R. Cai, C. Chen, The crown and the scepter: roles of the protein corona in nanomedicine, Adv. Mater. 1805740 (2018) 1–13, https://doi.org/10.1002/adma.201805740.
[5] M.P. Monopoli, D. Walczyk, A. Campbell, G. Elia, I. Lynch, F. Baldelli Bombelli, K.A. Dawson, Physical-chemical aspects of protein corona: relevance to in vitro and in vivo biological impacts of nanoparticles, J. Am. Chem. Soc. 133 (2011) 2525–2534, https://doi.org/10.1021/ja107583h.
[6] E. Casals, V.F. Puntes, Inorganic nanoparticle biomolecular corona: formation, evolution and biological impact, Nanomedicine 7 (2012) 1917–1930, https://doi.org/10.2217/nnm.12.169.
[7] S. Tenzer, D. Docter, J. Kuharev, A. Musyanovych, V. Fetz, R. Hecht, F. Schlenk, D. Fischer, K. Kiouptsi, C. Reinhardt, K. Landfester, H. Schild, M. Maskos, S.K. Knauer, R.H. Stauber, Rapid formation of plasma protein corona critically affects nanoparticle pathophysiology, Nat. Nanotechnol. 8 (2013) 772–781, https://doi.org/10.1038/nnano.2013.181.
[8] L. Vroman, A.L. Adams, G. Fischer, P. Munoz, Interaction of high molecular weight kininogen, factor XII, and fibrinogen in plasma at interfaces, Blood 55 (1980) 156–159.
[9] S. Shahabi, L. Treccani, R. Dringen, K. Rezwan, Modulation of silica nanoparticle uptake into human osteoblast cells by variation of the ratio of amino and Sulfonate surface groups: effects of serum, ACS Appl. Mater. Interfaces 7 (2015) 13821–13833, https://doi.org/10.1021/acsami.5b01900.
[10] A.C.G. Weiss, H.G. Kelly, M. Faria, Q.A. Besford, A.K. Wheatley, C.-S. Ang, E.J. Crampin, F. Caruso, S.J. Kent, Link between low-fouling and stealth: a whole blood biomolecular corona and cellular association analysis on nanoengineered particles, ACS Nano 13 (2019) 4980–4991, https://doi.org/10.1021/acsnano.9b00552.
[11] L. Ding, C. Yao, X. Yin, C. Li, Y. Huang, M. Wu, B. Wang, X. Guo, Y. Wang, M. Wu, Size, shape, and protein corona determine cellular uptake and removal mechanisms of gold nanoparticles, Small 14 (2018) 1–13, https://doi.org/10.1002/smll.201801451.
[12] D. Di Silvio, N. Rigby, B. Bajka, A. Mayes, A. Mackie, F. Baldelli Bombelli, Technical tip: high-resolution isolation of nanoparticle–protein corona complexes from physiological fluids, Nanoscale 7 (2015) 11980–11990, https://doi.org/10.1039/C5NR02618K.
[13] H. Moustaoui, J. Saber, I. Djeddi, Q. Liu, D. Movia, A. Prina-Mello, J. Spadavecchia, M. Lamy De La Chapelle, N. Djaker, A protein corona study by scattering correlation spectroscopy: a comparative study between spherical and urchin-shaped gold nanoparticles, Nanoscale 11 (2019) 3665–3673, https://doi.org/10.1039/c8nr09891c.
[14] C. Gräfe, M. von der Lühe, A. Weidner, P. Globig, J.H. Clement, S. Dutz, F.H. Schacher, Protein corona formation and its constitutional changes on magnetic nanoparticles in serum featuring a polydehydroalanine coating: effects of charge and incubation conditions, Nanotechnology 30 (2019) 265707, , https://doi.org/10.1088/1361-6528/ab0ed0.
[15] V. Mirshafiee, R. Kim, M. Mahmoudi, M.L. Kraft, The importance of selecting a proper biological milieu for protein corona analysis in vitro: human plasma versus human serum, Int. J. Biochem. Cell Biol. 75 (2016) 188–195, https://doi.org/10.1016/j.biocel.2015.11.019.
[16] M.H.-O. Rashid, S.F. Ralph, M.H.-O. Rashid, S.F. Ralph, Carbon nanotube membranes: synthesis, properties, and future filtration applications, Nanomaterials 7 (2017) 99, https://doi.org/10.3390/nano7050099.
[17] V. Gorshkov, J.A. Bubis, E.M. Solovyeva, M.V. Gorshkov, F. Kjeldsen, Protein corona formed on silver nanoparticles in blood plasma is highly selective and resistant to physicochemical changes of the solution, Environ. Sci. Nano. 6 (2019) 1089–1098, https://doi.org/10.1039/c8en01054d.
[18] S. Palchetti, D. Pozzi, A.L. Capriotti, G. La Barbera, R.Z. Chiozzi, L. Digiacomo, G. Peruzzi, G. Caracciolo, A. Laganà, Influence of dynamic flow environment on nanoparticle-protein corona: from protein patterns to uptake in cancer cells, Colloids Surf. B Biointerfaces 153 (2017) 263–271, https://doi.org/10.1016/j.colsurfb.2017.02.037.
[19] D. Walczyk, F.B. Bombelli, M.P. Monopoli, I. Lynch, K.A. Dawson, What the cell "sees" in bionanoscience, J. Am. Chem. Soc. 132 (2010) 5761–5768, https://doi.org/10.1021/ja910675v.
[20] S. Milani, F. Baldelli Bombelli, A.S. Pitek, K.A. Dawson, J. Rädler, Reversible versus irreversible binding of transferrin to polystyrene nanoparticles: soft and hard Corona, ACS Nano 6 (2012) 2532–2541, https://doi.org/10.1021/nn204951s.
[21] C. Weber, S. Morsbach, K. Landfester, Possibilities and limitations of different separation techniques for the analysis of the protein corona, Angew. Chemie Int. Ed. (2019), https://doi.org/10.1002/anie.201902323.
[22] E.V. Munsell, B. Fang, M.O. Sullivan, Histone-mimetic gold nanoparticles as versatile scaffolds for gene transfer and chromatin analysis, Bioconjug. Chem. 29 (2018) 3691–3704, https://doi.org/10.1021/acs.bioconjchem.8b00611.
[23] A.O. Luby, E.K. Breitner, K.K. Comfort, Preliminary protein corona formation stabilizes gold nanoparticles and improves deposition efficiency, Appl. Nanosci. 6 (2016) 827–836, https://doi.org/10.1007/s13204-015-0501-z.
[24] N. Bertrand, P. Grenier, M. Mahmoudi, E.M. Lima, E.A. Appel, F. Dormont, J.M. Lim, R. Karnik, R. Langer, O.C. Farokhzad, Mechanistic understanding of in vivo protein corona formation on polymeric nanoparticles and impact on pharmacokinetics, Nat. Commun. 8 (2017), https://doi.org/10.1038/s41467-017-00600-w.
[25] V. Mirshafiee, M. Mahmoudi, K. Lou, J. Cheng, M.L. Kraft, Protein corona significantly reduces active targeting yield, Chem. Commun. 49 (2013) 2557, https://doi.org/10.1039/c3cc37307j.
[26] M. Mahmoudi, S. Sheibani, A.S. Milani, F. Rezaee, M. Gauberti, R. Dinarvand, H. Vali, Crucial role of the protein corona for the specific targeting of nanoparticles, Nanomedicine 10 (2015) 215–226, https://doi.org/10.2217/nnm.14.69.
[27] C. Corbo, R. Molinaro, A. Parodi, N.E. Toledano Furman, F. Salvatore, E. Tasciotti, The impact of nanoparticle protein corona on cytotoxicity, immunotoxicity and target drug delivery, Nanomedicine 11 (2016) 81–100, https://doi.org/10.2217/nnm.15.188.
[28] C. Ge, J. Du, L. Zhao, L. Wang, Y. Liu, D. Li, Y. Yang, R. Zhou, Y. Zhao, Z. Chai, C. Chen, Binding of blood proteins to carbon nanotubes reduces cytotoxicity, Proc. Natl. Acad. Sci. 108 (2011) 16968–16973, https://doi.org/10.1073/pnas.1105270108.
[29] G. Duan, S.G. Kang, X. Tian, J.A. Garate, L. Zhao, C. Ge, R. Zhou, Protein corona mitigates the cytotoxicity of graphene oxide by reducing its physical interaction with cell membrane, Nanoscale 7 (2015) 15214–15224, https://doi.org/10.1039/c5nr01839k.
[30] M.S. Stan, L.O. Cinteza, L. Petrescu, M.A. Mernea, O. Calborean, D.F. Mihailescu, C. Sima, A. Dinischiotu, Dynamic analysis of the interactions between Si/SiO2 quantum dots and biomolecules for improving applications based on nano-bio interfaces, Sci. Rep. 8 (2018) 91–95, https://doi.org/10.1038/s41598-018-23621-x.
[31] A.B. Engin, A.W. Hayes, The impact of immunotoxicity in evaluation of the nanomaterials safety, Toxicol. Res. Appl. 2 (2018) 239784731875557, , https://doi.org/10.1177/2397847318755579.
[32] Z.J. Deng, M. Liang, M. Monteiro, I. Toth, R.F. Minchin, Nanoparticle-induced unfolding of fibrinogen promotes mac-1 receptor activation and inflammation, Nat. Nanotechnol. 6 (2011) 39–44, https://doi.org/10.1038/nnano.2010.250.
[33] C. Augustsson, K. Lundkvist, B. Dahlbäck, M. Lundqvist, S. Linse, T. Cedervall, M. Lilja, The nanoparticle protein corona formed in human blood or human blood fractions, PLoS One 12 (2017) e0175871, , https://doi.org/10.1371/journal.pone.0175871.
[34] V. Colapicchioni, M. Tilio, L. Digiacomo, V. Gambini, S. Palchetti, C. Marchini, D. Pozzi, S. Occhipinti, A. Amici, G. Caracciolo, Personalized liposome-protein corona in the blood of breast, gastric and pancreatic cancer patients, Int. J. Biochem. Cell Biol. 75 (2016) 180–187, https://doi.org/10.1016/j.biocel.2015.09.002.
[35] M.I. Setyawati, C.Y. Tay, D. Docter, R.H. Stauber, D.T. Leong, Understanding and exploiting nanoparticles' intimacy with the blood vessel and blood, Chem. Soc. Rev. 44 (2015) 8174–8199, https://doi.org/10.1039/C5CS00499C.
[36] M. Kokkinopoulou, J. Simon, K. Landfester, V. Mailänder, I. Lieberwirth, Visualization of the protein corona: towards a biomolecular understanding of nanoparticle-cell-interactions, Nanoscale 9 (2017) 8858–8870, https://doi.org/10.1039/c7nr02977b.
[37] M. Sun, L. Xu, J.H. Bahng, H. Kuang, S. Alben, N.A. Kotov, C. Xu, Intracellular localization of nanoparticle dimers by chirality reversal, Nat. Commun. 8 (2017) 1847, , https://doi.org/10.1038/s41467-017-01337-2.
[38] A. Krais, L. Wortmann, L. Hermanns, N. Feliu, M. Vahter, S. Stucky, S. Mathur, B. Fadeel, Targeted uptake of folic acid-functionalized iron oxide nanoparticles by ovarian cancer cells in the presence but not in the absence of serum, Nanomed. Nanotechnol. Biol. Med. 10 (2014) 1421–1431, https://doi.org/10.1016/j.nano.2014.01.006.

[39] D. Bargheer, J. Nielsen, G. Gébel, M. Heine, S.C. Salmen, R. Stauber, H. Weller, J. Heeren, P. Nielsen, The fate of a designed protein corona on nanoparticles in vitro and in vivo, Beilstein J. Nanotechnol. 6 (2015) 36–46, https://doi.org/10.3762/bjnano.6.5.

[40] M. Lunova, A. Prokhorov, M. Jirsa, M. Hof, A. Olzyńska, P. Jurkiewicz, Š. Kubinová, O. Lunov, A. Dejneka, Nanoparticle core stability and surface functionalization drive the mTOR signaling pathway in hepatocellular cell lines, Sci. Rep. 7 (2017) 1–16, https://doi.org/10.1038/s41598-017-16447-6.

[41] S. Palchetti, D. Caputo, L. Digiacomo, A.L. Capriotti, R. Coppola, D. Pozzi, G. Caracciolo, Protein corona fingerprints of liposomes: new opportunities for targeted drug delivery and early detection in pancreatic cancer, Pharmaceutics 11 (2019), https://doi.org/10.3390/pharmaceutics11010031.

[42] N. Ruthardt, D.C. Lamb, C. Bräuchle, Single-particle tracking as a quantitative microscopy-based approach to unravel cell entry mechanisms of viruses and pharmaceutical nanoparticles, Mol. Ther. 19 (2011) 1199–1211, https://doi.org/10.1038/mt.2011.102.

[43] L. Parhamifar, S.M. Moghimimbrane, Total internal reflection fluorescence (TIRF) microscopy for real-time imaging of nanoparticle-cell plasma membrane interaction, in: M. Soloviev (Ed.), Nanoparticles Biol. Med. Methods Protoc, Humana Press, Totowa, NJ, 2012, pp. 473–482, , https://doi.org/10.1007/978-1-61779-953-2.

[44] E.L. Elson, D. Magde, Fluorescence correlation spectroscopy. I. Conceptual basis and theory, Biopolymers 13 (1974) 1–27, https://doi.org/10.1002/bip.1974.360130102.

[45] D. Magde, E.L. Elson, W.W. Webb, Fluorescence correlation spectroscopy. II. An experimental realization, Biopolymers 13 (1974) 29–61, https://doi.org/10.1002/bip.1974.360130103.

[46] J.R. Lakowicz, Chapter 24. Fluorescence correlation spectroscopy, Princ. Fluoresc. Spectrosc, 3rd ed, Springer US, Boston, MA, 2006, pp. 797–840, , https://doi.org/10.1007/978-0-387-46312-4.

[47] S.A. Kim, K.G. Heinze, P. Schwille, Fluorescence correlation spectroscopy in living cells, Nat. Methods 4 (2007) 963–973, https://doi.org/10.1038/nmeth1104.

[48] P. Schwille, J. Bieschke, F. Oehlenschläger, Kinetic investigations by fluorescence correlation spectroscopy: the analytical and diagnostic potential of diffusion studies, Biophys. Chem. 66 (1997) 211–228, https://doi.org/10.1016/S0301-4622(97)00061-6.

[49] M. Eigen, R. Rigler, Sorting single molecules: application to diagnostics and evolutionary biotechnology, Proc. Natl. Acad. Sci. 91 (2006) 5740–5747, https://doi.org/10.1073/pnas.91.13.5740.

[50] K. Bacia, E. Haustein, P. Schwille, Fluorescence correlation spectroscopy: principles and applications, Cold Spring Harb Protoc (2014) (2014), https://doi.org/10.1101/pdb.top081802 pdb.top081802-pdb.top081802.

[51] P. Schwille, F.J. Meyer-Almes, R. Rigler, Dual-color fluorescence cross-correlation spectroscopy for multicomponent diffusional analysis in solution, Biophys. J. 72 (1997) 1878–1886, https://doi.org/10.1016/S0006-3495(97)78833-7.

[52] U. Meseth, T. Wohland, R. Rigler, H. Vogel, Resolution of fluorescence correlation measurements, Biophys. J. 76 (1999) 1619–1631, https://doi.org/10.1016/S0006-3495(99)77321-2.

[53] F. Mérola, O. Nüße, S. Dupré-Crochet, M. Tramier, M. Erard, D. Durand, L. Bouchab, C.S. Ziegler, F. Fieschi, Quantitative live-cell imaging and 3D modeling reveal critical functional features in the cytosolic complex of phagocyte NADPH oxidase, J. Biol. Chem. (2019), https://doi.org/10.1074/jbc.ra118.006864 jbc.RA118.006864.

[54] D. Krüger, J. Ebenhan, S. Werner, K. Bacia, Measuring protein binding to lipid vesicles by fluorescence cross-correlation spectroscopy, Biophys. J. 113 (2017) 1311–1320, https://doi.org/10.1016/j.bpj.2017.06.023.

[55] K. Bacia, S.A. Kim, P. Schwille, Fluorescence cross-correlation spectroscopy in living cells, Nat. Methods 3 (2006) 83–89, https://doi.org/10.1038/nmeth822.

[56] R. Rigler, Ü. Mets, J. Widengren, P. Kask, Fluorescence correlation spectroscopy with high count rate and low background: analysis of translational diffusion, Eur. Biophys. J. 22 (1993) 169–175, https://doi.org/10.1007/BF00185777.

[57] J. Ries, P. Schwille, New concepts for fluorescence correlation spectroscopy on membranes, Phys. Chem. Chem. Phys. 10 (2008) 3487–3497, https://doi.org/10.1039/b718132a.

[58] X. Zhang, A. Poniewierski, K. Sozański, Y. Zhou, A. Brzozowska-Elliott, R. Holyst, Fluorescence correlation spectroscopy for multiple-site equilibrium binding: a case of doxorubicin-DNA interaction, Phys. Chem. Chem. Phys. 21 (2019) 1572–1577, https://doi.org/10.1039/c8cp06752j.

[59] X. Zhang, A. Poniewierski, A. Jelińska, A. Zagozdzon, A. Wisniewska, S. Hou, R. Hołyst, Determination of equilibrium and rate constants for complex formation by fluorescence correlation spectroscopy supplemented by dynamic light scattering and Taylor dispersion analysis, Soft Matter 12 (2016) 8186–8194, https://doi.org/10.1039/c6sm01791f.

[60] W. Al-Soufi, B. Reija, M. Novo, S. Felekyan, R. Kühnemuth, C.A.M. Seidel, Fluorescence correlation spectroscopy, a tool to investigate supramolecular dynamics: inclusion complexes of pyronines with cyclodextrin, J. Am. Chem. Soc. 127 (2005) 8775–8784, https://doi.org/10.1021/ja0508976.

[61] C.E. Pinguet, J.M. Hoffmann, F.A. Plamper, E. Ryll, W. Richtering, A. Yaroslavov, D. Wöll, A.A. Steinschulte, M. Brugnoni, A. Sybachin, PEO-b-PPO star-shaped polymers enhance the structural stability of electrostatically coupled liposome/polyelectrolyte complexes, PLoS One 14 (2019) e0210898, , https://doi.org/10.1371/journal.pone.0210898.

[62] E. Sherman, A. Itkin, Y.Y. Kuttner, E. Rhoades, D. Amir, E. Haas, G. Haran, Using fluorescence correlation spectroscopy to study conformational changes in denatured proteins, Biophys. J. 94 (2008) 4819–4827, https://doi.org/10.1529/biophysj.107.120220.

[63] J.R. Larochelle, G.B. Cobb, A. Steinauer, E. Rhoades, A. Schepartz, Fluorescence correlation spectroscopy reveals highly efficient cytosolic delivery of certain penta-arg proteins and stapled peptides, J. Am. Chem. Soc. 137 (2015) 2536–2541, https://doi.org/10.1021/ja510391n.

[64] R.F. Wissner, A. Steinauer, S.L. Knox, A.D. Thompson, A. Schepartz, Fluorescence correlation spectroscopy reveals efficient cytosolic delivery of protein cargo by cell-Permeant miniature proteins, ACS Cent. Sci. 4 (2018) 1379–1393, https://doi.org/10.1021/acscentsci.8b00446.

[65] T.T. Le, S. Harlepp, C.C. Guet, K. Dittmar, T. Emonet, T. Pan, P. Cluzel, Real-time RNA profiling within a single bacterium, Proc. Natl. Acad. Sci. 102 (2005) 9160–9164, https://doi.org/10.1073/pnas.0503311102.

[66] K. Bacia, D. Scherfeld, N. Kahya, P. Schwille, Fluorescence correlation spectroscopy relates rafts in model and native membranes, Biophys. J. 87 (2004) 1034–1043, https://doi.org/10.1529/biophysj.104.040519.

[67] Y. Engström, K. Skouloudaki, D.K. Papadopoulos, P. Tomancak, L. Terenius, R. Rigler, C. Zechner, V. Vukojević, Control of Hox transcription factor concentration and cell-to-cell variability by an auto-regulatory switch, Development 146 (2019) dev168179, , https://doi.org/10.1242/dev.168179.

[68] M. Gösch, R. Rigler, Fluorescence correlation spectroscopy of molecular motions and kinetics, Adv. Drug Deliv. Rev. 57 (2005) 169–190, https://doi.org/10.1016/j.addr.2004.07.016.

[69] K. Bacia, P. Schwille, A dynamic view of cellular processes by in vivo fluorescence auto- and cross-correlation spectroscopy, Methods 29 (2003) 74–85, https://doi.org/10.1016/S1046-2023(02)00291-8.

[70] R.A. Murray, Y. Qiu, F. Chiodo, M. Marradi, S. Penadés, S.E. Moya, A quantitative study of the intracellular dynamics of fluorescently labelled glyco-gold nanoparticles via fluorescence correlation spectroscopy, Small 10 (2014) 2602–2610, https://doi.org/10.1002/smll.201303604.

[71] E. Hertz, L. Terenius, V. Vukojević, P. Svenningsson, GPR37 and GPR37L1 differently interact with dopamine 2 receptors in live cells, Neuropharmacology (2018) 1–7, https://doi.org/10.1016/j.neuropharm.2018.11.009.

[72] P. Schwille, Fluorescence correlation spectroscopy and its potential for intracellular applications, Cell Biochem. Biophys. 34 (2001) 383–408, https://doi.org/10.1385/CBB:34:3:383.

[73] S. Dominguez-Medina, S. Chen, J. Blankenburg, P. Swanglap, C.F. Landes, S. Link, Measuring the hydrodynamic size of nanoparticles using fluctuation correlation spectroscopy, Annu. Rev. Phys. Chem. 67 (2016) 489–514, https://doi.org/10.1146/annurev-physchem-040214-121510.

[74] J. Hühn, C. Fedeli, Q. Zhang, A. Masood, P. Del Pino, N.M. Khashab, E. Papini, W.J. Parak, Dissociation coefficients of protein adsorption to nanoparticles as quantitative metrics for description of the protein corona: a comparison of experimental techniques and methodological relevance, Int. J. Biochem. Cell Biol. 75 (2016) 148–161, https://doi.org/10.1016/j.biocel.2015.12.015.

[75] Y. Shen, J. Kim, E.F. Strittmatter, J.M. Jacobs, D.G. Camp, R. Fang, N. Tolié, R.J. Moore, R.D. Smith, Characterization of the human blood plasma proteome, Proteomics 5 (2005) 4034–4045, https://doi.org/10.1002/pmic.200401246.

[76] C. Röcker, M. Pötzl, F. Zhang, W.J. Parak, G.U. Nienhaus, A quantitative fluorescence study of protein monolayer formation on colloidal nanoparticles, Nat. Nanotechnol. 4 (2009) 577–580, https://doi.org/10.1038/nnano.2009.195.

[77] X. Jiang, S. Weise, M. Hafner, C. Röcker, F. Zhang, W.J. Parak, G.U. Nienhaus, Quantitative analysis of the protein corona on FePt nanoparticles formed by transferrin binding, J. R. Soc. Interface 7 (2010), https://doi.org/10.1098/rsif.2009.0272.focus.

[78] P. Maffre, K. Nienhaus, F. Amin, W.J. Parak, G.U. Nienhaus, Characterization of protein adsorption onto fept nanoparticles using dual-focus fluorescence correlation spectroscopy, Beilstein J. Nanotechnol. 2 (2011) 374–383, https://doi.org/10.3762/bjnano.2.43.

[79] D. Hühn, K. Kantner, C. Geidel, S. Brandholt, I. De Cock, S.J.H. Soenen, P. Riveragil, J.M. Montenegro, K. Braeckmans, K. Müllen, G.U. Nienhaus, M. Klapper, W.J. Parak, Polymer-coated nanoparticles interacting with proteins and cells: focusing on the sign of the net charge, ACS Nano 7 (2013) 3253–3263, https://doi.org/10.1021/nn3059295.

[80] C. Röcker, M. Pötzl, F. Zhang, W.J. Parak, G.U. Nienhaus, A quantitative fluorescence study of protein monolayer formation on colloidal nanoparticles, Nat. Nanotechnol. 4 (2009) 577–580, https://doi.org/10.1038/nnano.2009.195.

[81] R. Gref, M. Lück, P. Quellec, M. Marchand, E. Dellacherie, S. Harnisch, T. Blunk, R.H. Müller, “Stealth” corona-core nanoparticles surface modified by polyethylene glycol (PEG): influences of the corona (PEG chain length and surface density) and of the core composition on phagocytic uptake and plasma protein adsorption, Colloids Surf. B Biointerfaces 18 (2000) 301–313, https://doi.org/10.1016/S0927-7765(99)00156-3.

[82] B. Pelaz, P. Del Pino, P. Maffre, R. Hartmann, M. Gallego, S. Rivera-Fernández, J.M. De La Fuente, G.U. Nienhaus, W.J. Parak, Surface functionalization of nanoparticles with polyethylene glycol: effects on protein adsorption and cellular uptake, ACS Nano 9 (2015) 6996–7008, https://doi.org/10.1021/acsnano.5b01326.

[83] O. Vilanova, J.J. Mittag, P.M. Kelly, S. Milani, K.A. Dawson, J.O. Rädler, G. Franzese, Understanding the kinetics of protein-nanoparticle corona formation, ACS Nano 10 (2016) 10842–10850, https://doi.org/10.1021/acsnano.6b04858.

[84] L. Treuel, S. Brandholt, P. Maffre, S. Wiegele, L. Shang, G.U. Nienhaus, Impact of protein modification on the protein corona on nanoparticles and nanoparticle–cell interactions, ACS Nano 8 (2014) 503–513, https://doi.org/10.1021/nn405019v.

[85] Y. Liu, L. Xie, S. Pang, Q. Zhao, J. Wang, M. Cui, Z. Wang, Probing temperature- and pH-dependent binding between quantum dots and bovine serum albumin by fluorescence correlation spectroscopy, Nanomaterials 7 (2017) 93, https://doi.org/10.3390/nano7050093.

[86] K. Bacia, I.V. Majoul, P. Schwille, Probing the endocytic pathway in live cells using dual-color fluorescence cross-correlation analysis, Biophys. J. 83 (2002)

1184–1193, https://doi.org/10.1016/S0006-3495(02)75242-9.
[87] A. Silvestri, D. di Silvio, I. Llarena, marcello marelli, R. Murray, L. Lay, L. Polito, S.E. Moya, Influence of surface coating on the intracellular behaviour of gold nanoparticles: a fluorescence correlation spectroscopy study, Nanoscale (2017), https://doi.org/10.1039/C7NR04640E.
[88] D. Di Silvio, A. Silvestri, L. Lay, L. Polito, S.E. Moya, Impact of ConcanavalinA affinity in the intracellular fate of protein corona on glucosamine au nanoparticles, Sci. Rep. 8 (2018) 9046, , https://doi.org/10.1038/s41598-018-27418-w.
[89] P. Schwille, E. Haustein, Fluorescence correlation spectroscopy an introduction to its concepts and applications oup Max-Planck-Institute for Biophysical Chemistry Am Fassberg 11 D-37077 Göttingen, ResearchGate, 2001.
[90] K. Bacia, P. Schwille, Practical guidelines for dual-color fluorescence cross-correlation spectroscopy, Nat. Protoc. 2 (2007) 2842–2856, https://doi.org/10.1038/nprot.2007.410.